

Outage Performance of RIS-aided Cooperative FD-SWIPT-NOMA in Nakagami- m Channels

Wilson de Souza Junior and Taufik Abrão

Abstract

In this work we derive new analytical expressions for the outage probability (OP) of the downlink (DL) cooperative full-duplex (FD) simultaneous wireless information power transfer (SWIPT) non-orthogonal multiple access (NOMA) system aided by reconfigurable intelligent surfaces (RIS). The expressions for both the strongest and weakest NOMA users are devised assuming Nakagami- m channel fading. The derived analytical OP expressions are simple to compute yet accurate for a wide range of RIS passive elements configurations, energy harvesting (EH) coefficient, and residual self-interference (SI) levels, being extensively validated by numerical simulations, demonstrating the correctness and accuracy of the proposed analytical method. The OP expressions reveal how paramount is to mitigate the SI in the FD relay mode, since for reasonable values of residual SI coefficient ($\bar{\omega} \geq -13\text{dB}$), it is notable its detrimental effect over the system performance; hence, new SI reduction methods for FD relays are useful for low number of passive elements. Also, applying the proposed OP expressions to predict the behaviour of the RIS-NOMA system equipped with a higher number of passive elements ($N \geq 30$) reveals a substantial reduction of the SI effect, motivating the implementation of the cooperative FD communications. Furthermore, we found the asymptotic behavior of outage probability of both clustered users, as well as the equal diversity order for both users, given by $\frac{N\mu^2}{2-2\mu^2}$ if the fraction of the harvest energy $\rho = 0$ or 0 if $\rho \neq 0$, indicating the influence of channel parameters and number of RIS elements in the performance.

Index Terms

RIS, mMTC, NOMA, Outage Probability, Cooperative, SWIPT, Nakagami- m , URLLC.

I. INTRODUCTION

Among several highly important services addressed in the fifth generation (5G) wireless communication systems, and also predicted to be present in wireless communications systems beyond 5G, massive machine type communication (mMTC) is a use case scenario widely targeted due to the exponential increases of devices interconnected inside a network. Since the wireless networks have become denser, one of the challenges is to support heavy traffic. In recent studies in the literature, it has been proofed that *non-orthogonal multiple access* (NOMA) can be superior than the multiple access schemes as deployed in the past generations of cellular networks, including

This work was supported in part by the CAPES (Financial Code 001) and National Council for Scientific and Technological Development (CNPq) of Brazil under Grant 310681/2019-7.

W. Junior and T. Abrão are with the Department of Electrical Engineering (DEEL). State University of Londrina (UEL). Po.Box 10.011, CEP:86057-970, Londrina, PR, Brazil. Email: wilsoonjr98@gmail.com; taufik@uel.br

frequency division multiple access (FDMA), time division multiple access (TDMA), and code division multiple access (CDMA), which possibly may not be able to scale to meet such new 5G use cases demands.

NOMA can be regarded as an interesting candidate to overcome such challenges, once NOMA technology allows multiple users to transmit in the same resource block (RB), *e.g.*, the time-frequency RB, by superimposing the users in a non-orthogonal power-domain or code-domain manner, which can lead to higher spectral efficiency (SE) and energy efficiency (EE), than the usual *orthogonal multiple access* (OMA). By adopting NOMA, the successive interference cancellation (SIC) is paramount to distinguish the respective user's signal, being essential for NOMA to work suitably.

NOMA also can contribute significantly to improve the quality of service (QoS), which is an important metric in the communications systems. However, naturally, in a cellular system, the cell-edge users are often compromised due to its geographical position; hence, to improve fairness, the cell-edge users need to be allocated a large amount of resources, which can harm the QoS of the cell-center users. Cooperative communications can be viewed as a potential solution for this issue, once it can improve the data rate of the cell-edge users, enhancing the fairness in a cell-based network. Cooperative communications can be subdivided into two categories, namely user relaying and dedicated relaying. The integration of NOMA and cooperative user relaying has attracted significant attention mainly due to the natural matching, since the cell-edge user information is known to the cell-center users [1]. This scenario is very important as well, since the device-to-device (D2D) communication is one of the key technologies for next generations communication systems [2], [3]. Cooperative communications can be performed under two distinct modes, namely half-duplex (HD) and full-duplex (FD). The HD mode is known for sub-dividing the transmission time-block, which can degrade the SE, while the FD mode can be performed simultaneously at the cost of *self-interference* (SI) aggregation.

Although some gains can be obtained with cooperative communications, the deployment of such technology can be detrimental to the battery lifetime of the devices since inevitably it drains the battery of the cell-center users. *Simultaneous wireless information and power transfer* (SWIPT) is a promising and sustainable technology that can be useful to address this issue while enables the implementation of the Internet of Things (IoT) as well, since the IoT devices are usually limited with respect to the energy for relay cooperation. Moreover, SWIPT technique allows the devices to harvest energy from the ambient radio-frequency (RF) sources and re-use it to cooperate with the cell-edge users. SWIPT also can be implemented through two ways, the *power-splitting* (PS) and *time-switching* (TS) [4]. The PS-SWIPT protocol divides the received signal power from the base station (BS) into two parts, one for *information decoding* (ID), while the other is for *energy harvesting* (EH) purpose. On the other hand, the TS-SWIPT protocol, necessarily splits the time-slots to perform the ID and EH processes separately. In this work, we will adopt the PS-SWIPT protocol [5].

Recently, *reflecting intelligent surfaces* (RIS) are attracting research attention due to its capability of changing and customizing the wireless propagation environment, which can aid by supporting high system throughput and be useful in indoor/outdoor scenarios where dense obstacles are present, as a dense urban environment. The RIS is composed of scattering elements which specifically are artificial meta-material structures composed of adaptive composite material layers, which has the ability to reflect incident electromagnetic waves and can be configured in

order to increase the signal level in a specific direction for a priority user, and it is calling attention mainly due to its features: capacity of being sustainable, low-power consumption, enhance communications metrics, facility of implementation and installation, compatibility and low-cost.

Since the aforementioned technologies are promising candidates for future wireless communications systems, their deployment has been investigated in several works recently. In [6], the RIS-assisted NOMA system has been analytically validated in terms of outage probability (OP) in a scenario with two users. The paper demonstrated that deploying a RIS structure can substantially improve the OP metric. In [7], the authors shown that FD-NOMA achieves lower outage probability and larger ergodic sum rate than half-duplex in lower SNR. In [8], the authors evaluate the impact of the direct link of BS-users on the system performance, by comparing the RIS-aided scenario with the relay-aided scenario. In [9] the OP for RIS-NOMA network has been analyzed considering the impact of the (im)perfect SIC (pSIC & ipSIC). Moreover, in [10], the authors assessed the impact of RIS phase shifting design in the outage probability, ergodic capacity and bit error probability through two phase configurations: a random phase and coherent phase shifting. Besides, the OP for downlink IRS-assisted backscatter communications with NOMA is derived in [11], providing valuable insights. In [12], the outage probability of a RIS-aided NOMA system under hardware impairments has been analyzed analytically; the authors develop a closed-form for the OP. Moreover, very recently, novel OP expression for RIS-aided communication systems has been developed in [13]. The authors demonstrated that the end-to-end channel statistics for both weakest and strongest users in a *non-cooperative* RIS-aided NOMA system under Nakagami- m can be approximated by *Moment-Matching* (MM) technique with the Gamma random variable modeling. In [14], the author analyzed a RIS-aided cooperative NOMA scheme and proposed a algorithm to minimize the power consumption. The performance of a cooperative NOMA system has been analyzed in [5], [15], [16], [17], [18].

A. Motivation and Contributions

Although the works in [6], [8], [9], [12], [13] and [14] have provided solid studies in the OP of RIS-aided NOMA systems, the integration of RIS-aided in cooperative communications are still in their infancy. Motivated by the aforementioned facts, in this work we aim to investigate the potential benefits of combining these technologies. To the best of our knowledge, there is no existing work exploring the impact of the RIS deployment on the OP of RIS-aided cooperative FD-SWIPT-NOMA system operating under Nakagami- m fading channels. Herein, in order to completely assess the OP performance, we focus on a two-user scenario with perfect SIC and perfect knowing CSI at the BS, while most sophisticated scenarios (and performance metrics such as secrecy outage, sum rate, etc.) are out of the scope of this work, being considered in future researches.

In light of the above motivations and challenges, the main *contributions* of this work are threefold, and can be summarized as follows:

- We analyze a cooperative NOMA system scenario combined with the SWIPT technique adopting a non-linear energy harvesting model whose aim is to encourage the strongest user to cooperate with the weakest user without compromising itself in terms of data rate and battery lifetime. Besides, we investigate the use of RIS, aiming to identify its benefits and drawbacks operating under the scenario mentioned above.

- We derive novel expressions for the Outage Probability (OP) for the analyzed system. Since such expression is parameterized with respect to the system and channel parameters, the effect of each parameter can be effectively scanned as a function of the number of RIS elements.
- Finally, to gain further insight, we found asymptotic expressions at a high signal-to-noise ratio (SNR) for the OP of users 1 and 2, as well as the diversity order for the RIS FD-SWIPT-NOMA systems, confirming that the Nakagami- m parameters, as well as the number of RIS elements, impact the diversity order and the asymptotic outage probability of both users.

The adopted methodology allows us to assess analytically the RIS-aided cooperative SWIPT-NOMA performance, which is essential to predict how the system acts in practice.

Notation: ${}_pF_q(\cdot; \cdot; \cdot)$ is the generalized hypergeometric function; $X \sim \mathcal{CN}(\mu, \sigma^2)$ denotes a random variable X following a Complex Normal distribution with mean μ and variance σ^2 ; $X \sim \text{Gamma}(k, \delta)$ denotes a random variable following a Gamma distribution with shape parameter k and scale parameter δ ; the magnitude of a complex number z is expressed by $|z|$; $\arg(\cdot)$ denotes the argument of a complex number; $\text{diag}(\cdot)$ denotes the diagonal operator; vectors and matrices are represented by bold-face letters; F_x denotes the Cumulative Density Function (CDF) of X ; f_X denotes the Probability Density Function (PDF) of X ; $Pr(\cdot)$ presents probability;

II. SYSTEM MODEL

Let us consider a RIS-aided NOMA-cooperative network where a BS equipped with a single antenna, denoted by source, simultaneously serves via downlink transmission to two users. The transmission process is aided by a RIS with a total of N elements, as depicted in Fig. 1.

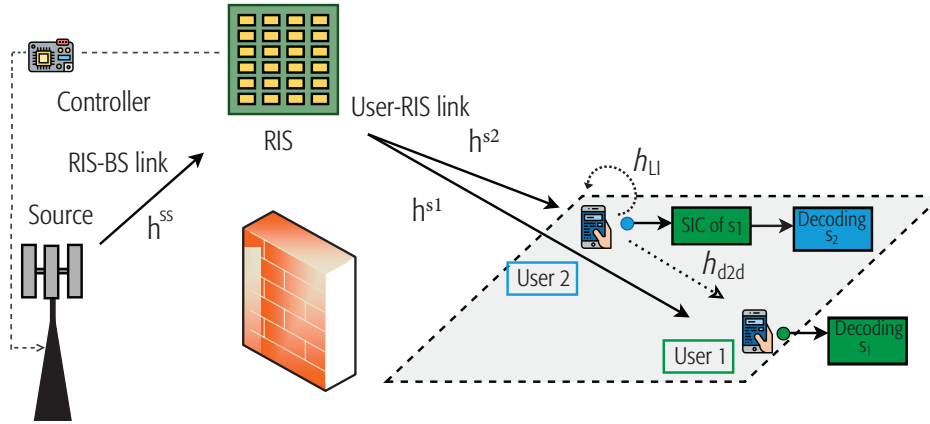


Fig. 1. System Model of a RIS-aided cooperative FD-SWIPT-NOMA.

The application scenarios for the system model illustrated in Fig. 1 are leveraged with the advent of IoT systems. The direct link between BS and user terminals (UTs) is assumed to be completely obstructed. However, the absence of a direct link in the adopted channel is representative and directly applicable to environments where the adoption of D2D communication can be really useful, *i.e.*, in offices, homes, etc. Furthermore, there is huge potential for application in industries and communication/automation between industrial robots.

To ensure QoS to the system, the user with better channel conditions can act as a cooperative relay adopting the decode-and-forward (DF) protocol [19], [20]. In order to reach ultra-low latency in the cooperative framework, a primordial feature in the 5G and 6G communication systems, in this work we have adopted that the cooperative user is equipped with two antennas, where the first one is responsible for receiving the signal and the other antenna to relaying [21]; hence, the cooperative process (at the user-relay) can occur in a FD mode [22], [23], [5], [18], [1].

In order to do not jeopardize the user with better channel conditions with respect to the battery lifetime, the user-relay can take advantage of the SWIPT technique by adopting the PS [24] [16] architecture where a fraction ρ of the received power and the remaining fraction $(1 - \rho)$ are simultaneously utilized to energy harvesting and to perform information decoding respectively. The energy harvested can be fully utilized to relay the rebuilt message version of the poor channel conditions user.

The RIS's properties can be represented by the phase-shift matrix:

$$\Theta = \text{diag}(\beta_1 e^{j\theta_1}, \beta_2 e^{j\theta_2}, \dots, \beta_N e^{j\theta_N})$$

where $\beta_n \in (0, 1]$ and $\theta_n \in [0, 2\pi]$ are the amplitude reflection coefficients and the phase-shift variables that can be optimized, respectively. We consider that the RIS is programmed by a dedicated controller (which is connected with the BS via a high-speed backhaul) [25] whose main aim is to update systematically the phase-shift at each coherence-time, once the phase-shift is directly related with the CSI. In this work we consider that all the amplitude coefficients are the same and with unity values $\beta_n = 1 \forall n = 1, \dots, N$.

We assume that all channels experience quasi-static flat fading over a coherence time and vary independently from one coherence time to another. For simplicity of analysis, in this work, the channel state information (CSI) is assumed to be perfectly known at the BS. The small-scale channel from the BS to the RIS is denoted by $\mathbf{h}^{ss} = [h_1^{ss}, h_2^{ss}, \dots, h_N^{ss}]^T \in \mathbb{C}^N$, while the small-scale channel between the RIS and the k -th user is denoted by $\mathbf{h}^{s,k} = [h_1^{s,k}, h_2^{s,k}, \dots, h_N^{s,k}]^T \in \mathbb{C}^N \forall k \in \{1, 2\}$. It is assumed that the magnitudes of $[\mathbf{h}^{ss}]_n = h_n^{ss}$ and $[\mathbf{h}^{s,k}]_n = h_n^{s,k}$ are independent RVs following the Nakagami- m ¹ distribution with shape parameters m_1 and m_2 , respectively, and spread parameters Ω_1 and Ω_2 , respectively, which are assumed the same values for all N elements of the RIS, while the phases are uniformly distributed in the range of $[0, 2\pi]$. In addition, in this work, the large-scale fading channel is adopted as $(\frac{d_0}{d})^\lambda$ [27] where d_0 corresponds to the reference distance, λ is the path-loss exponent and d is the distance between BS-RIS and RIS-Users.

Hence, the equivalent channel for the k -th user can be written as:

$$h_k = \mathbf{h}^{ss} \Theta \mathbf{h}^{s,k} \left(\frac{d_0}{d_{ss}}\right)^{\frac{\lambda}{2}} \left(\frac{d_0}{d_{s,k}}\right)^{\frac{\lambda}{2}}, \quad \forall k \in \{1, 2\}. \quad (1)$$

Similarly, the equivalent channel for D2D communication can be written as $h_{d2d} = \tilde{h}_{d2d} \left(\frac{d_0'}{d_{2,1}}\right)^{\frac{\lambda}{2}}$, where the term \tilde{h}_{d2d} is the channel between the strongest user and weakest user, which is modeled as a complex Normal distribution

¹One can notice that Nakagami- m distribution is a general form to represent both Rayleigh and Rician distributions. Further details can be found at [26] Section [3.2.2].

with zero mean and unity variance, *i.e.*, $\tilde{h}_{d2d} \sim \mathcal{CN}(0, 1)$.

It is worth to point that the optimal phase-shift of RIS elements for the case when the source and the users are equipped with just a single transmit and receiver antenna has been already studied in the literature, and its general solution can be given as $\theta_n = \tilde{\theta} - \arg(h_n^{ss} h_n^{s,k})$ [6], where $\tilde{\theta}$ is an arbitrary constant ranging in $[0, 2\pi)$. Herein, without loss of generality, we selected $\tilde{\theta} = 0$. Hence, the optimal phase-shift solution can be written as [28]:

$$\theta_n = -\arg(h_n^{ss}) - \arg(h_n^{s,k}).$$

For easiness of manipulation on the afterward equations, let us denote:

$$\begin{aligned} |h_k| &= \left| \mathbf{h}^{ss} \mathbf{\Theta} \mathbf{h}^{s,k} \left(\frac{d_0}{d_{ss}} \right)^{\frac{\lambda}{2}} \left(\frac{d_0}{d_{s,k}} \right)^{\frac{\lambda}{2}} \right| = \left| \left(\frac{d_0}{d_{ss}} \right)^{\frac{\lambda}{2}} \left(\frac{d_0}{d_{s,k}} \right)^{\frac{\lambda}{2}} \sum_{n=1}^N h_n^{ss} \beta_n e^{j\theta_n} h_n^{s,k} \right| \\ &= \left(\frac{d_0^2}{d_{ss} d_{s,k}} \right)^{\frac{\lambda}{2}} \underbrace{\sum_{n=1}^N h_n^{ss} h_n^{s,k}}_h, \quad \forall k \in \{1, 2\}. \end{aligned} \quad (2)$$

A. Signal Model

In NOMA, the source transmit a superimposed signal x that propagates from the source for the users through the RIS, with $x = \sqrt{\alpha_1} s_1 + \sqrt{\alpha_2} s_2$, where $\alpha_k \in (0, 1)$, $\forall k \in \{1, 2\}$ denotes the power allocation coefficients, with $\alpha_1 + \alpha_2 = 1$, $\alpha_1 > \alpha_2$ and $s_k \forall k \in \{1, 2\}$ is the message of k -th user, which is assumed without loss of generality $\mathbb{E}[|s_k|^2] = 1$.

1) *Strongest User*: The observation at the strongest user which will be designated for ID can be written as follows

$$y_2^{\text{ID}}(t) = \underbrace{h_2 \sqrt{P(1-\rho)} x(t)}_{\text{Superimposed info.}} + \underbrace{h_{\text{SI}} \sqrt{\rho P} \hat{x}_1(t-\tau)}_{\text{Self Interference}} + \underbrace{n_2(t)}_{\text{Noise}}, \quad (3)$$

where $0 \leq \rho \leq 1$ is the received power fraction utilized to energy harvesting and the SI term comes from by adopting the FD mode at the user-relay². In this work we consider that h_{SI} is free of fading due to the short distance transmission [30], and its power is given by $\bar{\omega}$, *i.e.*, $|h_{\text{SI}}|^2 = \bar{\omega}$, $\hat{x}_1(t-\tau)$ is the signal transmitted by the user-relay containing the decoded message \hat{s}_1 , τ denotes the processing delay (which is assumed that it is lower than the coherence time) at the user-relay caused by FD mode and n_2 is the Additive White Gaussian Noise (AWGN) at the user 2 (strongest user) with $n_2 \sim \mathcal{CN}(0, \sigma_2^2)$.

For the EH process, we employ a practical non-linear model [31]. Furthermore the power utilized in the relaying phase P_H and the energy harvested E_H at the user 2 are straightly connected and can be given by

$$P_H = \frac{E_H}{T} = \frac{\frac{P_{\max}}{1+e^{-a_2(P_{\text{in}}-a_3)}} - \frac{P_{\max}}{1+e^{a_2 a_3}}}{1 - \frac{1}{1+e^{a_2 a_3}}}}, \quad (4)$$

²Self-interference (SI) or loop-interference (LI) refers to the signal that are transmitted by the transmitter antenna of a FD node and looped back to the receiver antenna at the same node [29].

where T is the transmission block, P_{\max} is the maximum harvested power, a_2 and a_3 are constants related to the EH circuits as capacitance, resistance and diode turn-on voltage, and P_{in} is

$$P_{\text{in}} = \rho \cdot P \cdot |h_2|^2 \quad (5)$$

2) *Weakest User*: The observation at the user 1 (weakest user) can be written as follows

$$y_1(t) = \underbrace{h_1 \sqrt{P} x(t)}_{\text{Superimposed information}} + \underbrace{h_{d2d} \sqrt{\rho P} \hat{x}_1(t - \tau)}_{\text{Coop. Transmission}} + \underbrace{n_1(t)}_{\text{Noise}}, \quad (6)$$

where $n_1 \sim \mathcal{CN}(0, \sigma_1^2)$ is the AWGN at the weakest user.

B. Signal-Interference-to-Noise-Ratio

According to NOMA, strongest user receives a superimposed message y_2 from the BS-RIS, and through SIC³, strongest user can obtain its own message s_2 , while the weakest user treats user strongest's information s_2 as noise for decoding its own message s_1 . Therefore, the received SINR at the user 2 for detecting s_1 is given by

$$\text{SINR}_{u2}^{s_1} = \frac{|h_2|^2 (1 - \rho) \gamma \alpha_1}{|h_2|^2 (1 - \rho) \gamma \alpha_2 + |h_{\text{SI}}|^2 \rho \gamma + 1}, \quad (7)$$

where γ denote the SNR at BS $\gamma = \frac{P}{\sigma^2}$, where we consider that $\sigma_1^2 = \sigma_2^2 = \sigma^2$. After message s_1 is detected, it is eliminated from the received signal (3) by performing the SIC process, thus, the SINR at user 2 for detecting s_2 is given by

$$\text{SINR}_{u2}^{s_2} = \frac{|h_2|^2 (1 - \rho) \gamma \alpha_2}{\gamma \rho |h_{\text{SI}}|^2 + 1}. \quad (8)$$

At the weakest user, the received SINR to detect s_1 from BS-IRS and the received SNR to detect s_1 from strongest user can be expressed, respectively, by:

$$\text{SINR}_{u1,S}^{s_1} = \frac{|h_1|^2 \gamma \alpha_1}{|h_1|^2 \gamma \alpha_2 + 1}, \quad (9)$$

and

$$\text{SNR}_{u1,2}^{s_1} = P_H |h_{d2d}|^2. \quad (10)$$

By adopting maximum ratio combining (MRC) rule, the overall SINR at the user 1 is equivalent to the sum of two received SINR, *i.e.*, from BS-RIS link and user 2 link, which can be expressed as [18], [32], [17]:

$$\begin{aligned} \text{SINR}_{u1}^{s_1} &= \text{SINR}_{u1,S}^{s_1} + \text{SNR}_{u1,2}^{s_1} \\ &= \frac{|h_1|^2 \gamma \alpha_1}{|h_1|^2 \gamma \alpha_2 + 1} + P_H |h_{d2d}|^2. \end{aligned} \quad (11)$$

³Here we consider that the SIC process is performed perfectly, *i.e.*, we do not take into account an eventual residual error from this process.

III. SYSTEM PERFORMANCE ANALYSIS

In order to explore the cooperative users in NOMA scenarios, in this section we examine and derive new closed-form expressions for the *outage probability* (P_{out}) of two users, where we consider that target SINRs are determined by the users' QoS requirements. The outage probability metric is paramount to evaluate the reliability of the transmission in the 5G and 6G systems, specially in the URLLC use mode. Next, we derive two new close-form OP expressions, respectively, for the strongest and weakest users in power-domain NOMA scenarios.

A. Statistical Channel Characterization

Before proceeding to the outage probability derivation, it is paramount to characterize the channel statistically. Let X be an RV following a Gamma distribution parameterized by shape parameter k and scale parameter δ , with PDF and CDF respectively given by:

$$f_X(x; k, \delta) = \frac{1}{\Gamma(k)\delta^k} x^{k-1} e^{-\frac{x}{\delta}} \quad (12)$$

$$F_X(x; k, \delta) = \frac{1}{\Gamma(k+1)} \left(\frac{x}{\delta}\right)^k {}_1F_1(k, k+1; -\frac{x}{\delta}) \quad (13)$$

The following lemma can be stated:

Lemma 1. *The distribution of channel $h = \sum_{n=1}^N h_n^{ss} h_n^{s,k}$ given in (2) can be approximated accurately by Gamma distribution $h \stackrel{\text{approx.}}{\sim} \text{Gamma}(k, \delta)$ via Moment-Matching technique [33], whose shape parameter k and scale parameter δ are given, respectively, by*

$$k = \frac{N\mu^2}{1-\mu^2}; \quad \delta = \frac{(1-\mu^2)}{\mu} \quad (14)$$

with μ given as

$$\mu = \frac{\Gamma(m_1 + \frac{1}{2})\Gamma(m_2 + \frac{1}{2})}{\Gamma(m_1)\Gamma(m_2)\sqrt{m_1 m_2}} \quad (15)$$

Proof. The proof is available in Lemma 2 of [13]. ■

Next, the outage probability of user 2 and user 1 for RIS-Aided cooperative SWIPT-NOMA systems are discussed in the following two sub-sections.

B. Strongest User Outage Probability

Particularly, the outage behavior for the strongest NOMA users occurs since user 2 cannot detect effectively the user 1' message by the SIC process and its message consequently or when the SIC process is performed successfully

but an error occurs to decode user 2' message. Mathematically it can be formulated by the union of the following events:

$$\begin{aligned}
P_{\text{out}}^{\text{U}_2} &= \Pr(\text{SINR}_{\text{U}_2}^{s_1} < \tilde{\gamma}_1) + \Pr(\text{SINR}_{\text{U}_2}^{s_1} \geq \tilde{\gamma}_1, \text{SINR}_{\text{U}_2}^{s_2} < \tilde{\gamma}_2) \\
&= \Pr\left(\frac{|h_2|^2(1-\rho)\gamma\alpha_1}{|h_2|^2(1-\rho)\gamma\alpha_2 + |h_{\text{SI}}|^2\rho\gamma + 1} < \tilde{\gamma}_1\right) + \\
&\Pr\left(\frac{|h_2|^2(1-\rho)\gamma\alpha_1}{|h_2|^2(1-\rho)\gamma\alpha_2 + |h_{\text{SI}}|^2\rho\gamma + 1} \geq \tilde{\gamma}_1, \right. \\
&\quad \left. \frac{|h_2|^2(1-\rho)\gamma\alpha_2}{|h_{\text{SI}}|^2\rho\gamma + 1} < \tilde{\gamma}_2\right), \tag{16}
\end{aligned}$$

where $\tilde{\gamma}_1 = 2^{R_1} - 1$ and $\tilde{\gamma}_2 = 2^{R_2} - 1$, with R_1 and R_2 being the target rates of the user 1 and user 2, respectively.

Theorem 1. *The closed-form expression for the outage probability of user 2 in RIS-aided cooperative FD-SWIPT-NOMA system is given in (17), at the top of next page, where k and δ are the Gamma distribution parameters given by (14) and $\varepsilon = \frac{\tilde{\gamma}_1 + \tilde{\gamma}_1\tilde{\gamma}_2}{\tilde{\gamma}_2}$.*

$$P_{\text{out}}^{\text{U}_2} = \begin{cases} \frac{\left(\left(\frac{d_{ss}d_{s,2}}{d_0^2}\right)^\lambda \frac{\tilde{\gamma}_1(\bar{\omega}\rho\gamma+1)}{(1-\rho)\gamma(\alpha_1-\tilde{\gamma}_1\alpha_2)} \frac{1}{\delta^2}\right)^{k/2}}{\Gamma(k+1)} {}_1F_1\left(k, k+1; -\frac{1}{\delta}\sqrt{\left(\frac{d_{ss}d_{s,2}}{d_0^2}\right)^\lambda \frac{\tilde{\gamma}_1(\bar{\omega}\rho\gamma+1)}{(1-\rho)\gamma(\alpha_1-\tilde{\gamma}_1\alpha_2)}}\right) & \text{if } \frac{\alpha_1}{\alpha_2} < \varepsilon \\ \frac{\left(\left(\frac{d_{ss}d_{s,2}}{d_0^2}\right)^\lambda \frac{\tilde{\gamma}_2(\bar{\omega}\rho\gamma+1)}{(1-\rho)\gamma\alpha_2} \frac{1}{\delta^2}\right)^{k/2}}{\Gamma(k+1)} {}_1F_1\left(k, k+1; -\frac{1}{\delta}\sqrt{\left(\frac{d_{ss}d_{s,2}}{d_0^2}\right)^\lambda \frac{\tilde{\gamma}_2(\bar{\omega}\rho\gamma+1)}{(1-\rho)\gamma\alpha_2}}\right) & \text{otherwise.} \end{cases} \tag{17}$$

Proof. The proof is provided in Appendix A ■

Corollary 1. *The Outage Probability for RIS-aided cooperative FD-SWIPT-NOMA systems under Rayleigh fading is given in (17) where k becomes $\hat{k} \triangleq \frac{N\hat{\mu}^2}{1-\hat{\mu}^2}$ and δ becomes $\hat{\delta} \triangleq \frac{(1-\hat{\mu}^2)}{\hat{\mu}}$ with $\hat{\mu} = \Gamma(\frac{3}{2})^2$.*

Proof. Due to the versatility of Nakagami- m distribution, it can be reduced to multiple types of channel fading, when m_1 and m_2 of \mathbf{h}^{ss} and $\mathbf{h}^{s,k}$ are set to one, i.e., $m_1 = m_2 = 1$, the Nakagami- m fading degrades to Rayleigh fading. By setting $m_1 = m_2 = 1$ in (15) and applying it in (14) the proof is completed. ■

Proposition 1. *Since the high-SNR behavior can be useful to further understand the capability of the analyzed system, we derive the asymptotic outage probability for user 2 $P_{\text{out}}^{\text{U}_2, \infty}$, and it is given by (18).*

Proof. By utilizing ${}_1F_1(k, k+1; a + \frac{1}{\gamma}) \approx {}_1F_1(k, k+1; a)$ in high SNR regime in (17), leads to (18). ■

$$P_{\text{out}}^{U_2, \infty} = \begin{cases} \frac{\left(\left(\frac{d_{ss} d_{s,2}}{d_0^2} \right)^\lambda \frac{\tilde{\gamma}_1 (\bar{\omega} \rho \gamma + 1)}{(1-\rho) \gamma (\alpha_1 - \tilde{\gamma}_1 \alpha_2)} \frac{1}{\delta^2} \right)^{k/2}}{\Gamma(k+1)} {}_1F_1 \left(k, k+1; -\frac{1}{\delta} \sqrt{\left(\frac{d_{ss} d_{s,2}}{d_0^2} \right)^\lambda \frac{\tilde{\gamma}_1 \bar{\omega} \rho}{(1-\rho) (\alpha_1 - \tilde{\gamma}_1 \alpha_2)}} \right) & \text{if } \frac{\alpha_1}{\alpha_2} < \varepsilon \\ \frac{\left(\left(\frac{d_{ss} d_{s,2}}{d_0^2} \right)^\lambda \frac{\tilde{\gamma}_2 (\bar{\omega} \rho \gamma + 1)}{(1-\rho) \gamma \alpha_2} \frac{1}{\delta^2} \right)^{k/2}}{\Gamma(k+1)} {}_1F_1 \left(k, k+1; -\frac{1}{\delta} \sqrt{\left(\frac{d_{ss} d_{s,2}}{d_0^2} \right)^\lambda \frac{\tilde{\gamma}_2 \bar{\omega} \rho}{(1-\rho) \alpha_2}} \right) & \text{otherwise.} \end{cases} \quad (18)$$

Corollary 2. To gain more insights, the diversity order can be evaluated based on the above analytical results. In the RIS-Aided cooperative FD-SWIPT-NOMA system, the **diversity order** for the user 2 is given by

$$\mathcal{D}_{U_2} = \frac{N\mu^2}{2-2\mu^2}, \text{ if } \rho = 0; \quad \text{or} \quad \hat{\mathcal{D}}_{U_2} = 0, \text{ if } \rho \neq 0 \quad (19)$$

Proof. The diversity order is defined as

$$\mathcal{D} = -\lim_{\gamma \rightarrow \infty} \frac{\log(P_{\text{out}}(\gamma))}{\log(\gamma)}, \quad (20)$$

Upon substituting (18) into (20) and after some manipulations, the diversity order for the user 2 is obtained. ■

Remark 1. Corollary 2 reveals useful insights. First, the diversity order when $\rho = 0$ is parameterized w.r.t. the Nakagami- m fading parameters and the number of reflecting elements of RIS, confirming that high reliability can be potentialized by larges RIS. Furthermore, exploring the channel parameters m_1 and m_2 can also boost the outage probability. Besides, when $\rho \neq 0$, the diversity order is zero, lower than when user two does not act as a relay; hence, a worse performance is expected for the former case.

C. Weakest User Outage Probability

In this case, the outage behavior for the weakest users occurs since user 2 cannot detect effectively the user 1' message neither user 1 can decode its own message or when user 2 detect the user 1' message but user 1 cannot detect its message after the MRC.

$$\begin{aligned} P_{\text{out}}^{U_1} &= \Pr(\text{SINR}_{U_2}^{s_1} < \tilde{\gamma}_1) + \Pr(\text{SINR}_{U_2}^{s_1} \geq \tilde{\gamma}_1, \text{SINR}_{U_1}^{s_1} < \tilde{\gamma}_1) \\ &= \Pr \left(\frac{|h_2|^2 (1-\rho) \gamma \alpha_1}{|h_2|^2 (1-\rho) \gamma \alpha_2 + |h_{SI}|^2 \rho \gamma + 1} < \tilde{\gamma}_1 \right) + \\ &\quad \Pr \left(\frac{|h_2|^2 (1-\rho) \gamma \alpha_1}{|h_2|^2 (1-\rho) \gamma \alpha_2 + |h_{SI}|^2 \rho \gamma + 1} \geq \tilde{\gamma}_1, \right. \\ &\quad \left. \frac{|h_1|^2 \gamma \alpha_1}{|h_1|^2 \gamma \alpha_2 + 1} + P_H |h_{d2d}|^2 < \tilde{\gamma}_1 \right) \end{aligned} \quad (21)$$

Theorem 2. The closed-form expression for the outage probability of user 1 in RIS-aided cooperative FD-SWIPT-NOMA system is given in (22), where

$$f(x) = e^{-K_3(\tilde{\gamma}_1 - x)} \frac{1}{x^2} \left(\frac{x}{\alpha_1 - \alpha_2 x} \right)^{\frac{k+2}{2}} e^{-K_2 \sqrt{\frac{x}{\alpha_1 - \alpha_2 x}}},$$

and the constants are computed as

$$K_1 = \frac{\alpha_1}{2\Gamma(k)} \left(\frac{1}{\gamma\delta^2} \left(\frac{d_{ss}d_{s,1}}{d_0^2} \right)^\lambda \right)^{k/2},$$

$$K_2 = \sqrt{\frac{1}{\gamma\delta^2} \left(\frac{d_{ss}d_{s,1}}{d_0^2} \right)^\lambda}, \quad \text{and} \quad K_3 = \frac{1}{P_{\max}} \left(\frac{d_{2,1}}{d_0'} \right)^k.$$

$$P_{\text{out}}^{\text{U}_1} = \begin{cases} \frac{\left(\left(\frac{d_{ss}d_{s,1}}{d_0^2} \right)^\lambda \frac{\tilde{\gamma}_1}{\gamma(\alpha_1 - \tilde{\gamma}_1\alpha_2)} \frac{1}{\delta^2} \right)^{k/2}}{\Gamma(k+1)} {}_1F_1 \left(k, k+1; -\frac{1}{\delta} \sqrt{\left(\frac{d_{ss}d_{s,1}}{d_0^2} \right)^\lambda \frac{\tilde{\gamma}_1}{\gamma(\alpha_1 - \tilde{\gamma}_1\alpha_2)}} \right), & \text{if } \rho = 0 \\ P_{\text{out}}^{\text{U}_2} + (1 - P_{\text{out}}^{\text{U}_2}) K_1 \left[\frac{2}{\alpha_1 k} \left(\frac{\tilde{\gamma}_1}{(\alpha_1 - \alpha_2 \tilde{\gamma}_1)} \right)^{k/2} {}_1F_1 \left(k, k+1; -K_2 \sqrt{\frac{\tilde{\gamma}_1}{(\alpha_1 - \alpha_2 \tilde{\gamma}_1)}} \right) - \sum_{\ell=0}^{L_1} f(\tilde{\gamma}_1 x_\ell + \tilde{\gamma}_1) w_\ell \right] & \rho > 0 \end{cases} \quad (22)$$

Proof. Please refer to Appendix B. ■

Remark 2. The Corollary 1 can be directly applied into Theorem 2 in order to obtain the outage probability for user 1 with Rayleigh fading.

Proposition 2. The asymptotic outage probability for user 1 $P_{\text{out}}^{\text{U}_1, \infty}$ is expressed as (23).

$$P_{\text{out}}^{\text{U}_1, \infty} = \begin{cases} \frac{\left(\left(\frac{d_{ss}d_{s,1}}{d_0^2} \right)^\lambda \frac{\tilde{\gamma}_1}{(1-\rho)\gamma(\alpha_1 - \tilde{\gamma}_1\alpha_2)} \frac{1}{\delta^2} \right)^{k/2}}{\Gamma(k+1)}, & \text{if } \rho = 0 \\ P_{\text{out}}^{\text{U}_2, \infty} + (1 - P_{\text{out}}^{\text{U}_2, \infty}) \left[\frac{2}{\alpha_1 k} \left(\frac{\tilde{\gamma}_1}{(\alpha_1 - \alpha_2 \tilde{\gamma}_1)} \right)^{k/2} - \sum_{\ell=0}^{L_1} f(\tilde{\gamma}_1 x_\ell + \tilde{\gamma}_1) w_\ell \right] & \rho > 0 \end{cases} \quad (23)$$

Proof. To proof Proposition 2, we utilized the approximation in eq. (22), in the next page, for the hypergeometric function ${}_1F_1(k, k+1; \frac{1}{\gamma}) \approx 1$, as well as set constants K_1 and K_2 above to $K_1 \approx K_2 \approx 0$ when $\gamma \rightarrow \infty$, completing the proof. ■

Corollary 3. *The diversity order in the RIS-aided cooperative FD-SWIPT-NOMA system for user 1 are given by $\mathcal{D}_{U_1} = \frac{N\mu^2}{2-2\mu^2}$ and $\hat{\mathcal{D}}_{U_1} = 0$ if $\rho = 0$ and $\rho \neq 0$ respectively.*

Proof. The proof is similar to the proof of Corollary 2. ■

Table I summarizes the analytical findings for the diversity order \mathcal{D} of user U1 (weakest) and U2 (strongest) in RIS-aided cooperative FD-SWIPT-NOMA system.

TABLE I
DIVERSITY ORDER \mathcal{D} FOR RIS-AIDED COOPERATIVE FD-SWIPT-NOMA SYSTEM

	User 1 (U_1)	User 2 (U_2)
$\rho = 0$	$\frac{N\mu^2}{2-2\mu^2}$	$\frac{N\mu^2}{2-2\mu^2}$
$\rho \neq 0$	0	0

IV. SIMULATION RESULTS

In this section, we aim to confirm through Monte-Carlo simulations the accuracy of our previous mathematical analysis and illustrate the achievable enhanced performance of the RIS-aided cooperative FD-SWIPT-NOMA system. The simulations results are averaged over 10^6 realizations. Unless stated otherwise, the parameters adopted are presented in Table II. In the following numerical results, the outage probability of user 2 and user 1 are depicted in blue and red color respectively, the Monte-Carlo simulations (MCS) is labeled as "Monte-Carlo" and the derived analytical expressions are labeled as "Analytical".

TABLE II
ADOPTED SIMULATION PARAMETERS.

Parameter	Value
RIS-aided Cooperative FD-SWIPT-NOMA system	
SNR @ BS	$\gamma = \frac{P}{\sigma^2} \in [0; 60]$ [dB]
# Reflecting Meta-Surfaces	$N \in \{5 : 50\}$
Power Allocation coefficients	$\alpha_1 = 0.6, \alpha_2 = 0.4$
Target Rate	$R_1 = R_2 = 1$ [BPCU]
The Distance from BS to RIS	$d_{ss} = 100$ [m]
The Distance from RIS to U_i	$d_{s,i} = 15, 10$ [m]
The Distance between Users	$d_{2,1} = 5$ [m]
Residual Self-Interference	$\bar{\omega} = -\{13, 20, 25, 30\}$ [dB]
EH coefficient	$\rho \in [0 : 0.1 : 1]$
Maximum harvested power	$P_{\max} = 1$ [W]
EH model constants	$a_2 = 150; a_3 = 0.014$
Channel Parameters	
Channel Model (BS-RIS/RIS-User)	Nakagami- m
Shape Parameter BS-RIS	$m_1 = 3$
Shape Parameter RIS-Users	$m_2 = 2$
Spread Parameter	$\Omega_1 = \Omega_2 = 1$
Reference Distance	$d_0 = 5$ [m]; $d_0' = 1$ [m]
Path Loss Exponent	$\lambda = 3.76, \kappa = 2$
Channel Model (D2D)	$\tilde{h}_{d2d} \sim \mathcal{CN}(0,1)$

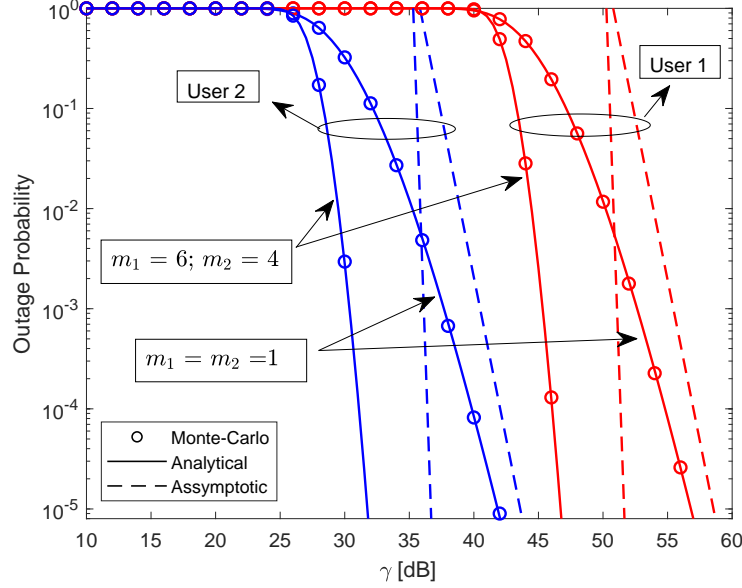


Fig. 2. Outage Probability performance over an RIS-aided cooperative FD-SWIPT-NOMA system with $N = 8$ passive reflecting elements with $\rho = 0$.

Fig. 2 depicts the OP of both users in a RIS-aided cooperative FD-SWIPT-NOMA system, with respect to the SNR (γ) by considering $R_1 = R_2 = 1$. One can notice that our proposed OP expressions provided in Theorem 1 and 2, given by Eq. (17) and Eq. (22), fitted very well with the MCS results in all SNR range analysed, since they matched properly, corroborating the correctness and accuracy of our analytical approach. Furthermore, the asymptotic behavior derived in eq. (18) and (23), and formulated by Proposition 1 and 2, respectively, reveals to be very accurate in high-SNR regime, as expected. Elaborating further, Fig. 2 covers two scenarios: *a*) for Nakagami- m parameters $m_1 = 6$ and $m_2 = 4$, and *b*) for $m_1 = m_2 = 1$ under energy harvesting (EH) coefficient $\rho = 0$, *i.e.*, the strongest user does not dedicate part of its received energy to acts as relay aiming to improve the weakest user conditions. Notably, when the Nakagami parameters are different from unity, the OP is substantially reduced compared with the case where they are unitary, and consequently, degrades to Rayleigh links. The reason for this behavior is due to the presence of LoS component in generalized Nakagami- m channels, which can improve remarkably the system performance, depending on m_1 and m_2 values. Hence, Fig. 2 confirms such scenarios where both BS-RIS and RIS-users links are in fact links Nakagami performing better than both Rayleigh links.

Fig. 3 reveals the impact of full-duplex self-interference $\bar{\omega}$ on the OP of user 2. Since user 2 is the most prejudiced due to the SI to perform directly over it and once the OP for user 1 also depends on the OP of the user 2, herein we just depict the OP for user 2. With $N = 20$ elements, Fig. 3 highlights how paramount is to mitigate the value of the SI, since it is notable its deleterious influence over the $P_{\text{out}}^{U_2}$, leading to a OP floor for $\bar{\omega} \geq -13$ dB. Hence, the development of new FD-SI technologies for SI reduction, leading to low-values of $\bar{\omega}$, can be very useful. On the other hand, one finding is that when the RIS is composed with a great number of elements, say $N \geq 30$, it can proportionate substantial SI mitigation in FD mode, motivating the implementation of the FD cooperative communications, and making it possible to reach a degree of reliability than $(1 - 10^{-4})$ till to lower values of $\bar{\omega}$.

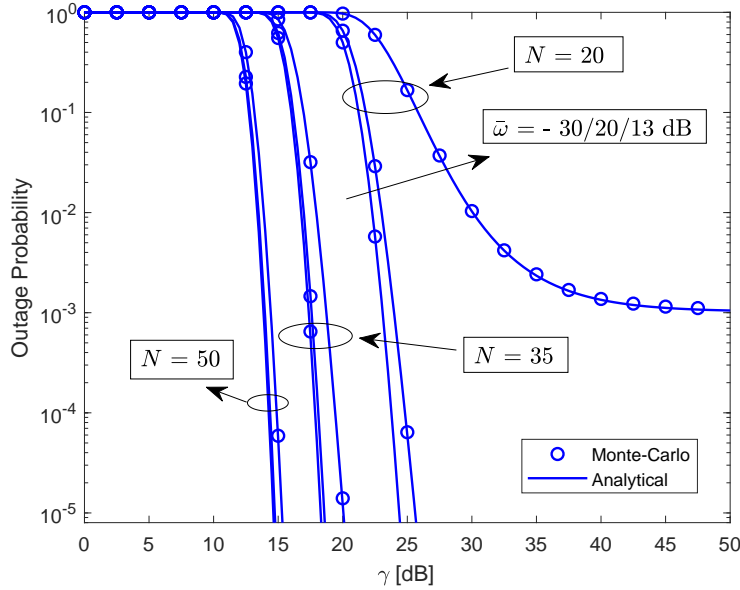


Fig. 3. Outage Probability for User 2 over an RIS-aided cooperative FD-SWIPT-NOMA system with different values of $\bar{\omega}$ and N for $\rho = 0.1$.

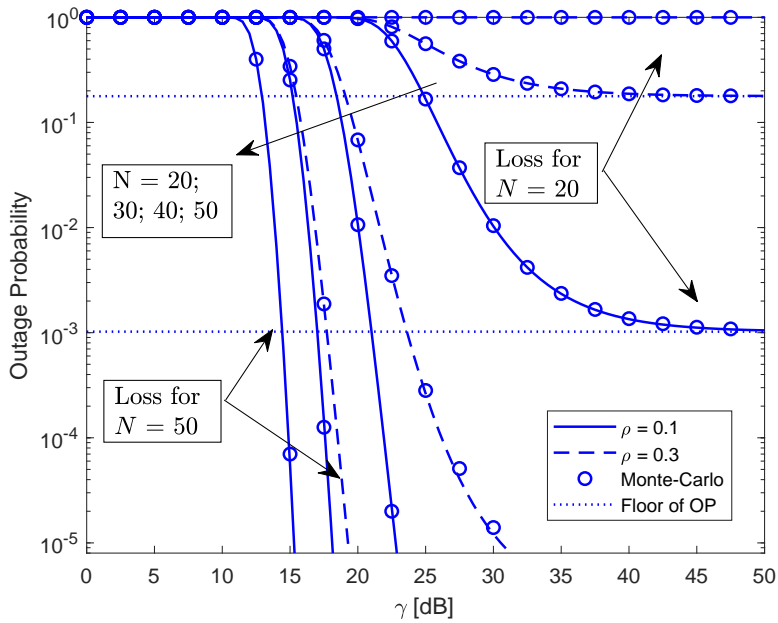


Fig. 4. Outage Probability for User 2 over an RIS-aided cooperative FD-SWIPT-NOMA system with different values of ρ and N for $\bar{\omega} = -13$ dB.

Fig. 4 depicts the OP behavior for user 2 when ρ increases for different values of N . As expected, the OP increases for increasing ρ , since the user 2 is dedicating a greater amount of its power to relay, simultaneously increasing the SI as well as decreasing the ID power. Furthermore, one can notice that for high values of N , the loss/gain is lower/higher than for low values of N , indicating the promising integration of RIS technologies in FD cooperative communications.

Finally, Fig. 3 and 4 jointly confirm that under high SNR regime ($\gamma \rightarrow \infty$), considering low values of N and high values of ρ or $\bar{\omega}$, the OP performance for the user 2 remarkable attains the analytical OP floor limit (blue dotted lines).

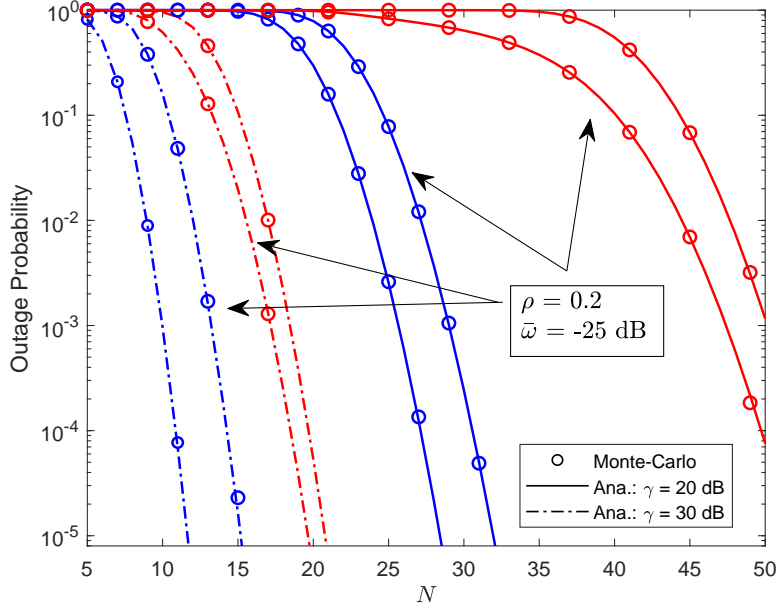


Fig. 5. Outage Probability for User 1 (red) and User 2 (blue) parameterized in the number of RIS elements (N), for $\gamma \in [20; 30]$ dB.

Fig. 5 illustrates the OP behavior of both users with respect to N . Firstly, we can see that for $\gamma = 30$ dB the curves are lower than the curves for $\gamma = 20$ dB, indicating that the OP for high SNR are lower than for low SNR as expected. Furthermore, we can see that for $\rho = 0$, to reach the same OP of 10^{-4} the user 2 needs $N = 10$ for $\gamma = 30$ dB, while for $\gamma = 20$ dB needs almost three times, $N = 28$, that is, by increasing 18 elements at the RIS we can reduce the power consumption in ten times. Regarding user 1, it is need to increase 30 RIS elements to get a performance lower than 10^{-3} . Secondly, we can see that the impact of cooperative communications in the low-SNR scenario is higher than those in high-SNR scenario, where it is justified due to the fact that in high-SNR regime the signal from cooperative communications is saturated due to the P_{\max} , while in low-SNR regime the signal coming from BS-RIS link can be "comparable" with that coming from the user 2.

Fig. 6.a) and 6.b) depict the OP for the strongest and weakest user, respectively, when N varies from 5 to 50 elements, and $\rho \in [0; 1]$ under two operation SNRs, $\gamma = 30$ dB and $\gamma = 20$ dB. Firstly, two extreme cases are of interest: $\rho = 0$ and $\rho = 1$; for the case $\rho = 0$, the user 2 does not act as relay, hence, its OP is as lower as possible independently of values of N . In the case $\rho = 1$, meaning that user 2 is relaying with all the power harvested, that is, the power for ID is zero, so naturally its OP is always in outage and consequently the user 1 is in outage as well, for any value of N . In between, when ρ increases from 0 to 1, we see that the OP for the weakest user for a fixed N decreases till some value and so remains constant, indicating that to harvest further an amount of power will not impact positively on the performance. After some steps increasing ρ , the OP of user 1 starts to increase again. It is justified by the fact that user 2 can harvest a maximum power P_{\max} and so it saturates (due to the non-linear

energy harvest model E_H in eq. (4)), and after increasing ρ the OP of user 1 increases due to the increase of OP of user 2.

Besides, Fig. 6 reveals that when $\gamma = 30$ dB, for $N \geq 20$ and $\rho \leq 0.5$ the user 2 can attain values for OP $\leq 10^{-4}$, similarly, when $N \geq 20$ and $\rho \leq 0.5$, the user 1 also can get OP lower than 10^{-4} . Differently, for a lower SNR, $\gamma = 20$ dB, the user 2 can obtain the same OP for $N \geq 30$ and $\rho \leq 0.2$ while the weakest user can obtain the same OP for $N \geq 50$ and $0.1 \leq \rho \leq 0.7$, indicating that the weakest user is more sensible to a change in the SNR. Furthermore, Fig. 6 demonstrates the versatility and accuracy of the proposed analytical OP expressions, eqs. (17) and (22), for the couple weakest-strongest users in RIS-aided cooperative FD-SWIPT-NOMA systems.

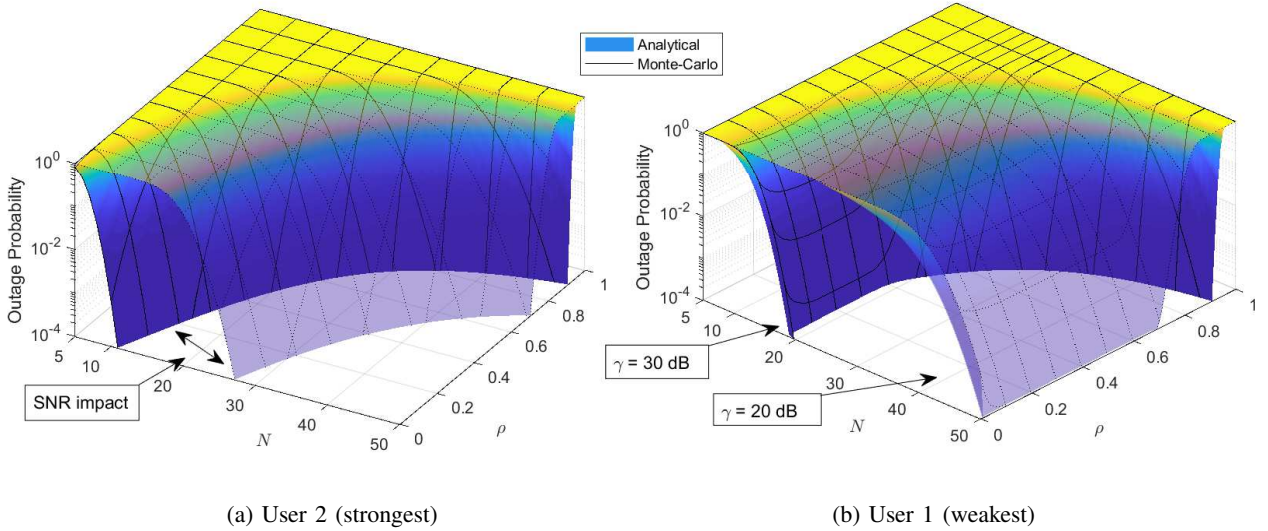


Fig. 6. Simulated and analytical OP performance results for the User 1 and User 2 over an RIS-aided FD-NOMA-Cooperative system parameterized in $N \in [5; 50]$ passive RIS elements, and EH coefficient $\rho \in [0; 1]$ for $\gamma = 30$ dB and $\gamma = 20$ dB. The NL-EH parameters are defined here as $a_2 = 0.8$ and $a_3 = 0.003$.

The outage probability for user 1 when it starts to move away from user 2 (distance $d_{2,1}$ in meters) is depicted in Fig. 7; the path-loss exponent from BS-RIS link is defined as $\lambda = 3$ and the path-loss exponent from the user's links is defined as $\kappa = 2$. One can see that by increasing the number of N from 20 to 50, the distance between the users also can be increased by 10 meters keeping the same outage probability order of 3×10^{-4} . Furthermore, the cooperative gain is higher for $N = 20$ than for $N = 50$ elements.

Finally, Fig. 8 depicts the outage probability for user 2 when N increases, as well as P_{\max} increases. One can infer that the cooperative gain increases as P_{\max} increases, however, we can see that it tend to be bounded for $P_{\max} \rightarrow \infty$. Furthermore, we can see that for $P_{\max} < 500$ mW, user 2 still can obtain an outage probability less than 10^{-4} when $N \geq 33$ elements, indicating that it can be applied to low-power low-complexity devices scenarios, as in IoT networks.

V. CONCLUSIONS

In this work we propose new analytical expressions for the outage probability in the DL of RIS-aided cooperative FD-SWIPT NOMA system assuming Nakagami- m statistics. The analytical OP expressions for both the strongest

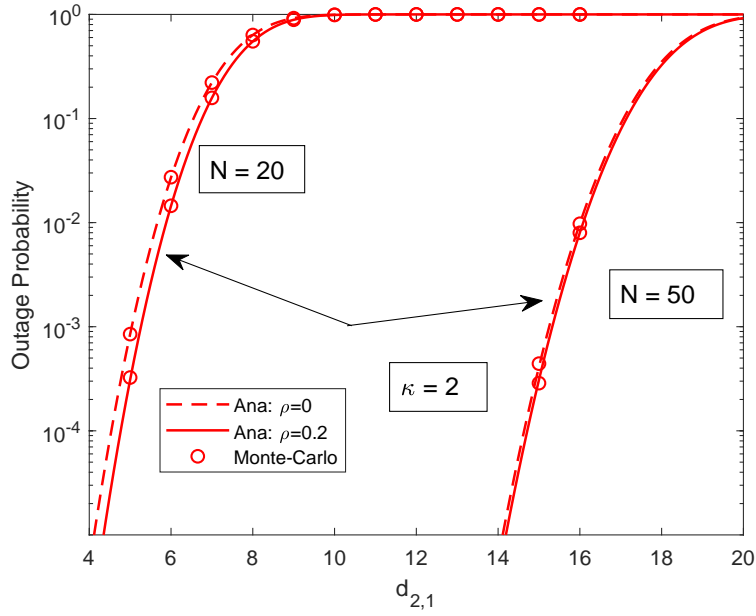


Fig. 7. Simulated and analytical OP performance results for the User 1 over an RIS-aided FD-NOMA-Cooperative system parameterized in the distance between the users $d_{2,1}$ for $\gamma = 15$ dB. The NL-EH parameters are defined here as $a_2 = 0.8$ and $a_3 = 0.003$.

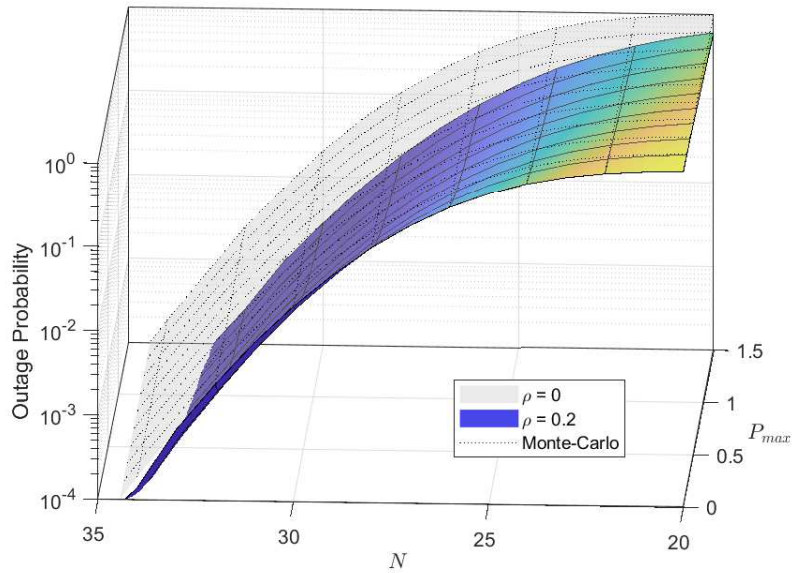


Fig. 8. Analytical and simulated OP for the User 2 over an RIS-aided FD-NOMA-Cooperative system with $\rho = 0$ and $\rho = 0.2$, $P_{\max} \in [1\text{mW}; 1.5\text{W}]$, and $\gamma = 19$ dB.

and weakest NOMA users are simple to compute yet accurate for a wide range of RIS passive elements (N), EH coefficient (ρ), and residual self-interference level ($\bar{\omega}$), being extensively validated by the numerical simulations. Also, the methodology shows that by increasing the number of passive elements, the OP for both types of users can be notably boosted in *non-cooperative* NOMA schemes, while by considering the cooperative schemes, a great number of passive elements ($N \geq 30$) can mitigate substantially the residual SI effect.

Furthermore, we found the asymptotic behavior of outage probability for both users, as well as the diversity order, given by $\frac{N\mu^2}{2-2\mu^2}$ if $\rho = 0$, and 0 if $\rho \neq 0$, indicating the influence of channel parameters and number of RIS elements on the system performance. Moreover, we have investigated the effect of the distance between the users; we conclude that by deploying a RIS the distance BS-user can be increased in tens of meters without performance degradation, indicating higher flexibility and reliability in cooperative communications applications.

Lastly, our analytical findings reveal that cooperative communications can be boosted by deploying RIS-aided cooperative FD-SWIPT technologies for NOMA systems. Since this work focused on a setting of one antenna at the BS, perfect CSI and perfect SIC, the impact of deployment of multi-antennas, imperfect SIC on the RIS phase-shift design and OP performance in FD-SWIPT-NOMA cooperative communications is a interesting research direction to be investigated in future works.

ACKNOWLEDGMENT

This work has been partially supported by the National Council for Scientific and Technological Development (CNPq) of Brazil under Grant 310681/2019-7 and CAPES (Scholarship). All the agencies are gratefully acknowledged.

APPENDIX A

PROOF OF THEOREM 1

After some manipulations, Eq. (16) can be written as

$$P_{\text{out}}^{\text{U}_2} = \Pr\left(h_2 < \sqrt{\zeta_{s2w}}\right) + \Pr\left(h_2 \geq \sqrt{\zeta_{s2w}}, h_2 < \sqrt{\zeta_{s2s}}\right), \quad (24)$$

where ζ_{s2w} and ζ_{s2s} are auxiliary variables given by:

$$\zeta_{s2w} = \frac{\tilde{\gamma}_1 (|h_{LI}|^2 \rho \gamma + 1)}{(1 - \rho) \gamma (\alpha_1 - \tilde{\gamma}_1 \alpha_2)}, \quad (25)$$

and

$$\zeta_{s2s} = \frac{\tilde{\gamma}_2 (|h_{LI}|^2 \rho \gamma + 1)}{(1 - \rho) \gamma \alpha_2}. \quad (26)$$

It is noteworthy that the second term in the right side of (24) will not exist in the case that $\zeta_{s2w} \geq \zeta_{s2s}$ which is equivalent to $\frac{\alpha_1}{\alpha_2} \leq \varepsilon$, with $\varepsilon = \frac{\tilde{\gamma}_1 + \tilde{\gamma}_1 \tilde{\gamma}_2}{\tilde{\gamma}_2}$. Furthermore, the second term in the right side of (24), can be written

as

$$\begin{aligned} & \Pr \left(h_2 \geq \sqrt{\zeta_{s2w}}, h_2 < \sqrt{\zeta_{s2s}} \right) = \\ & \Pr \left(h_2 < \sqrt{\zeta_{s2s}} \right) - \Pr \left(h_2 < \sqrt{\zeta_{s2w}} \right), \end{aligned} \quad (27)$$

in this way, by utilizing (2) and (27) in (24), the outage probability of the U_2 is given as

$$P_{\text{out}}^{U_2} = \begin{cases} \Pr \left(h < \sqrt{\left(\frac{d_{ss}d_{s,2}}{d_0^2} \right)^\lambda \zeta_{s2w}} \right) & \text{if } \frac{\alpha_1}{\alpha_2} \leq \varepsilon, \\ \Pr \left(h < \sqrt{\left(\frac{d_{ss}d_{s,2}}{d_0^2} \right)^\lambda \zeta_{s2s}} \right) & \text{otherwise.} \end{cases} \quad (28)$$

Hence with the aid of Lemma 1, the outage probability of the strongest user is straightforwardly obtained as (17) by utilizing (13) into (28), and considering $|h_{LI}|^2 = \bar{\omega}$ so the proof is completed. ■

APPENDIX B

PROOF OF THEOREM 2

To derive the outage probability of the weakest user it is reasonable to separate it in two cases, *i.e.*, when the strongest user does not operate as relay ($\rho = 0$), and when the strongest user operates as a relay ($\rho \neq 0$).

I) $\rho = 0$ (strongest user does not act as a relay)

After some manipulations and utilizing the methods similar to the Appendix A, we can written (21) as

$$\begin{aligned} P_{\text{out}}^{U_1} &= \Pr \left(h < \sqrt{\zeta'_{s2w} \left(\frac{d_{ss}d_{s,1}}{d_0^2} \right)^\lambda} \right) + \\ & \Pr \left(h \geq \sqrt{\zeta'_{s2w} \left(\frac{d_{ss}d_{s,1}}{d_0^2} \right)^\lambda}, h < \sqrt{\zeta_{w2w} \left(\frac{d_{ss}d_{s,1}}{d_0^2} \right)^\lambda} \right) \\ &= \Pr \left(h < \sqrt{\zeta'_{s2w} \left(\frac{d_{ss}d_{s,1}}{d_0^2} \right)^\lambda} \right), \end{aligned} \quad (29)$$

where

$$\zeta'_{s2w} = \zeta_{w2w} = \frac{\tilde{\gamma}_1}{\gamma(\alpha_1 - \tilde{\gamma}_1\alpha_2)}. \quad (30)$$

By utilizing (13) into (29), (22)-(a) is obtained.

II) $\rho \neq 0$ (strongest user operates as a relay)

By analyzing the second argument in the right size of (21):

$$\underbrace{\frac{|h_1|^2\gamma\alpha_1}{|h_1|^2\gamma\alpha_2 + 1}}_{X_1} + \underbrace{P_H|h_{d2d}|^2}_{X_2} < \tilde{\gamma}_1, \quad (31)$$

let us denote the first and second term in the left side of the inequality above as two random variables, namely X_1 and X_2 , hence

$$X_1 + X_2 < \tilde{\gamma}_1. \quad (32)$$

Notice that in NOMA systems the end-to-end channels h_1-h_2 are correlated, once it has the same component h_{ss} (link from BS to the RIS) and this fact hinders the process of obtaining a close-form expression for the P_{out} when the strongest user acts as relay; herein, we aim to find some approximations that lead to precise and correct analysis.

Since X_1 and X_2 are correlated random variables, it is very hard, if not impossible, to derive the exact statistic characterization of the joint distribution of both r.v.. To circumvent this difficulty, we will consider $P_H \approx P_{\text{max}}$, which is a reasonable adoption at the higher the SNR γ , indicating that harvested energy is very near to the saturation value P_{max} . So, we can evaluate the PDF of X_2 as follows

$$\Pr(P_{\text{max}}|h_{d2d}|^2 < z) = F_{\tilde{h}_{d2d}} \left(\sqrt{\frac{z}{P_{\text{max}}} \left(\frac{d_{2,1}}{d_0'} \right)^\kappa} \right). \quad (33)$$

Since $\tilde{h}_{d2d} \sim \mathcal{CN}(0, 1)$, $|\tilde{h}_{d2d}| \sim \mathcal{R}(\sqrt{0.5})$, hence by differentiating (33), we obtain that X_2 follows an exponential distribution with rate parameter given by $\frac{1}{P_{\text{max}}} \left(\frac{d_{2,1}}{d_0'} \right)^\kappa$, whose PDF is written as

$$f_{X_2} = \frac{1}{P_{\text{max}}} \left(\frac{d_{2,1}}{d_0'} \right)^\kappa \exp \left[-z \frac{1}{P_{\text{max}}} \left(\frac{d_{2,1}}{d_0'} \right)^\kappa \right] \quad (34)$$

Furthermore, the CDF of X_1 is obtained similarly

$$\Pr \left(\frac{|h_1|^2 \gamma \alpha_1}{|h_1|^2 \gamma \alpha_2 + 1} < z \right) = F_h \left(\sqrt{\frac{z}{\gamma(\alpha_1 - z\alpha_2)} \left(\frac{d_{ss}d_{s,1}}{d_0^2} \right)^\lambda} \right)$$

since f_{X_1} is obtained by differentiating (35), it is obtain after some mathematical manipulations

$$\begin{aligned} f_{X_1}(z) &= \frac{\alpha_1}{2\Gamma(k)} \left(\frac{1}{\gamma\delta^2} \left(\frac{d_{ss}d_{s,1}}{d_0^2} \right)^\lambda \right)^{k/2} \frac{1}{z^2} \left(\frac{z}{\alpha_1 - \alpha_2 z} \right)^{\frac{k+2}{2}} \\ &\times \exp \left[-\sqrt{\frac{z}{\gamma\delta^2(\alpha_1 - \alpha_2 z)} \left(\frac{d_{ss}d_{s,1}}{d_0^2} \right)^\lambda} \right]. \end{aligned} \quad (35)$$

Hence, the OP for the weakest user when the strongest acts as relay is computed by (21), and can be expressed as

$$P_{\text{out}}^{\text{U}_1} = P_{\text{out}}^{\text{U}_2} + (1 - P_{\text{out}}^{\text{U}_2}) \times \Pr(X_1 + X_2 < \tilde{\gamma}_1), \quad (36)$$

where the last term can be computed as follows

$$\begin{aligned} \Pr(X_1 + X_2 < \tilde{\gamma}_1) &= \int_0^{\tilde{\gamma}_1} F_{X_2}(\tilde{\gamma}_1 - x) f_{X_1}(x) dx \\ &= K_1 \left(\underbrace{\int_0^{\tilde{\gamma}_1} \frac{1}{x^2} \left(\frac{x}{\alpha_1 - \alpha_2 x} \right)^{\frac{k+2}{2}} e^{-K_2 \sqrt{\frac{x}{\alpha_1 - \alpha_2 x}}} dx}_{I_1} \right. \\ &\quad \left. - \underbrace{\int_0^{\tilde{\gamma}_1} e^{-K_3(\tilde{\gamma}_1 - x)} \frac{1}{x^2} \left(\frac{x}{\alpha_1 - \alpha_2 x} \right)^{\frac{k+2}{2}} e^{-K_2 \sqrt{\frac{x}{\alpha_1 - \alpha_2 x}}} dx}_{I_2} \right) \end{aligned} \quad (37)$$

with $K_3 = \frac{1}{P_{\max}} \left(\frac{d_{2,1}}{d_0'} \right)^\kappa$, $K_1 = \frac{\alpha_1}{2\Gamma(k)} \left(\frac{1}{\gamma\delta^2} \left(\frac{d_{ss}d_{s,1}}{d_0^2} \right)^\lambda \right)^{k/2}$, $K_2 = \sqrt{\frac{1}{\gamma\delta^2} \left(\frac{d_{ss}d_{s,1}}{d_0^2} \right)^\lambda}$. After some change of variables, I_1 can be written as

$$\begin{aligned} I_1 &= 2\alpha_2^{-k/2} \alpha_1^{-1} \int_0^{\sqrt{\frac{\alpha_2 \tilde{\gamma}_1}{\alpha_1 - \alpha_2 \tilde{\gamma}_1}}} x^{k-1} e^{-\frac{K_2}{\sqrt{\alpha_2}} x} dx \\ &\stackrel{(a)}{=} \frac{2}{\alpha_1 k} \left(\sqrt{\frac{\tilde{\gamma}_1}{\alpha_1 - \alpha_2 \tilde{\gamma}_1}} \right)^k \times \\ &\quad \times {}_1F_1 \left(k, k+1; -K_2 \sqrt{\frac{\tilde{\gamma}_1}{\alpha_1 - \alpha_2 \tilde{\gamma}_1}} \right) \end{aligned} \quad (38)$$

where in (a) we resort to [34, Eq. (3.381.1)] and [34, Eq. (9.236.4)].

Term I_2 can be approximated by Laguerre-Quadrature

$$I_2 \approx \sum_{\ell=0}^{L_1} f(\tilde{\gamma}_1 x_\ell + \tilde{\gamma}_1) w_\ell, \quad (39)$$

where w_ℓ are the weights given by $w_\ell = \frac{2}{(1-x_\ell^2)[P_n'(x_\ell + \tilde{\gamma}_1)]^2}$ [35], P_n' is the derivative of the n -th Legendre polynomial, x_ℓ are the roots of the n -th Legendre polynomial and $f(x) = e^{-K_3(\tilde{\gamma}_1 - x)} \frac{1}{x^2} \left(\frac{x}{\alpha_1 - \alpha_2 x} \right)^{\frac{k+2}{2}} e^{-K_2 \sqrt{\frac{x}{\alpha_1 - \alpha_2 x}}}$. Therefore, the Outage Probability of the user 1 when $\rho \neq 0$, is obtained by substituting (38) and (39) into (37) and plugging into (36). ■

REFERENCES

- [1] M. Zeng, W. Hao, O. A. Dobre, and Z. Ding, "Cooperative noma: state of the art, key techniques, and open challenges," *IEEE Network*, vol. 34, no. 5, pp. 205–211, 2020.
- [2] W. Jiang, B. Han, M. A. Habibi, and H. D. Schotten, "The road towards 6g: A comprehensive survey," *IEEE Open Journal of the Communications Society*, vol. 2, pp. 334–366, 2021.
- [3] N. H. Mahmood, H. Alves, O. A. López, M. Shehab, D. P. M. Osorio, and M. Latva-Aho, "Six key features of machine type communication in 6g," in *2020 2nd 6G Wireless Summit (6G SUMMIT)*, 2020, pp. 1–5.
- [4] N. Ashraf, S. A. Sheikh, S. A. Khan, I. Shaya, and M. Jalal, "Simultaneous wireless information and power transfer with cooperative relaying for next-generation wireless networks: A review," *IEEE Access*, vol. 9, pp. 71 482–71 504, 2021.
- [5] T.-N. Tran, T. P. Vo, P. Fazio, and M. Voznak, "Swipt model adopting a ps framework to aid iot networks inspired by the emerging cooperative noma technique," *IEEE Access*, vol. 9, pp. 61 489–61 512, 2021.

- [6] Y. Cheng, K. H. Li, Y. Liu, K. C. Teh, and H. V. Poor, "Downlink and uplink intelligent reflecting surface aided networks: Noma and oma," *IEEE Transactions on Wireless Communications*, vol. 20, no. 6, pp. 3988–4000, 2021.
- [7] X. Yue, Y. Liu, S. Kang, A. Nallanathan, and Z. Ding, "Exploiting full/half-duplex user relaying in noma systems," *IEEE Transactions on Communications*, vol. 66, no. 2, pp. 560–575, 2018.
- [8] A.-T. Le, N.-D. X. Ha, D.-T. Do, A. Silva, and S. Yadav, "Enabling user grouping and fixed power allocation scheme for reconfigurable intelligent surfaces-aided wireless systems," *IEEE Access*, vol. 9, pp. 92 263–92 275, 2021.
- [9] X. Yue and Y. Liu, "Performance analysis of intelligent reflecting surface assisted noma networks," *IEEE Transactions on Wireless Communications*, pp. 1–1, 2021.
- [10] D. Selimis, K. P. Peppas, G. C. Alexandropoulos, and F. I. Lazarakis, "On the performance analysis of ris-empowered communications over nakagami-m fading," *IEEE Communications Letters*, vol. 25, no. 7, pp. 2191–2195, 2021.
- [11] S. Li, L. Bariah, S. Muhaidat, A. Wang, and J. Liang, "Outage analysis of noma-enabled backscatter communications with intelligent reflecting surfaces," *IEEE Internet of Things Journal*, pp. 1–1, 2022.
- [12] A. Hemanth, K. Umamaheswari, A. C. Pogaku, D.-T. Do, and B. M. Lee, "Outage performance analysis of reconfigurable intelligent surfaces-aided noma under presence of hardware impairment," *IEEE Access*, vol. 8, pp. 212 156–212 165, 2020.
- [13] B. Tahir, S. Schwarz, and M. Rupp, "Analysis of uplink irs-assisted noma under nakagami-m fading via moments matching," *IEEE Wireless Communications Letters*, vol. 10, no. 3, pp. 624–628, 2021.
- [14] J. Zuo, Y. Liu, and N. Al-Dhahir, "Reconfigurable intelligent surface assisted cooperative non-orthogonal multiple access systems," *IEEE Transactions on Communications*, pp. 1–1, 2021.
- [15] P. Hüu, M. A. Arfaoui, S. Sharafeddine, C. M. Assi, and A. Ghayeb, "A low-complexity framework for joint user pairing and power control for cooperative noma in 5g and beyond cellular networks," *IEEE Transactions on Communications*, vol. 68, no. 11, pp. 6737–6749, 2020.
- [16] T. N. Do and B. An, "Optimal sum-throughput analysis for downlink cooperative swipt noma systems," in *2018 2nd International Conference on Recent Advances in Signal Processing, Telecommunications Computing (SigTelCom)*, 2018, pp. 85–90.
- [17] X. Yue, Y. Liu, S. Kang, A. Nallanathan, and Z. Ding, "Outage performance of full/half-duplex user relaying in noma systems," in *2017 IEEE International Conference on Communications (ICC)*, 2017, pp. 1–6.
- [18] W. Wu, X. Yin, P. Deng, T. Guo, and B. Wang, "Transceiver design for downlink swipt noma systems with cooperative full-duplex relaying," *IEEE Access*, vol. 7, pp. 33 464–33 472, 2019.
- [19] D. Wan, M. Wen, F. Ji, Y. Liu, and Y. Huang, "Cooperative noma systems with partial channel state information over nakagami-m fading channels," *IEEE Transactions on Communications*, vol. 66, no. 3, pp. 947–958, 2017.
- [20] L. Wei, R. Q. Hu, Y. Qian, and G. Wu, "Enable device-to-device communications underlying cellular networks: challenges and research aspects," *IEEE Communications Magazine*, vol. 52, no. 6, pp. 90–96, 2014.
- [21] Y. Alsaba, C. Y. Leow, and S. K. A. Rahim, "Full-duplex cooperative non-orthogonal multiple access with beamforming and energy harvesting," *IEEE Access*, vol. 6, pp. 19 726–19 738, 2018.
- [22] H. Huang and M. Zhu, "Energy efficiency maximization design for full-duplex cooperative noma systems with swipt," *IEEE Access*, vol. 7, pp. 20 442–20 451, 2019.
- [23] Q. Y. Liau and C. Y. Leow, "Cooperative noma system with virtual full duplex user relaying," *IEEE Access*, vol. 7, pp. 2502–2511, 2018.
- [24] K. M. Rabie, A. Salem, E. Alsusa, and M.-S. Alouini, "Energy-harvesting in cooperative af relaying networks over log-normal fading channels," in *2016 IEEE International Conference on Communications (ICC)*, 2016, pp. 1–7.
- [25] T. N. Do, G. Kaddoum, T. L. Nguyen, D. B. da Costa, and Z. J. Haas, "Multi-ris-aided wireless systems: Statistical characterization and performance analysis," *arXiv preprint arXiv:2104.01912*, 2021.
- [26] A. Goldsmith, *Wireless communications*. Cambridge university press, 2005.
- [27] J. Tang, J. Luo, J. Ou, X. Zhang, N. Zhao, D. K. C. So, and K.-K. Wong, "Decoupling or learning: joint power splitting and allocation in mc-noma with swipt," *IEEE Transactions on Communications*, vol. 68, no. 9, pp. 5834–5848, 2020.
- [28] A.-A. A. Boulogeorgos and A. Alexiou, "Ergodic capacity analysis of reconfigurable intelligent surface assisted wireless systems," in *2020 IEEE 3rd 5G World Forum (5GWF)*. IEEE, 2020, pp. 395–400.
- [29] Z. Zhang, Z. Ma, M. Xiao, Z. Ding, and P. Fan, "Full-duplex device-to-device-aided cooperative nonorthogonal multiple access," *IEEE Transactions on Vehicular Technology*, vol. 66, no. 5, pp. 4467–4471, 2016.
- [30] B. Xu, Z. Xiang, P. Ren, and X. Guo, "Outage performance of downlink full-duplex network-coded cooperative noma," *IEEE Wireless Communications Letters*, vol. 10, no. 1, pp. 26–29, 2021.

- [31] E. Boshkovska, D. W. K. Ng, N. Zlatanov, and R. Schober, "Practical non-linear energy harvesting model and resource allocation for swipt systems," *IEEE Communications Letters*, vol. 19, no. 12, pp. 2082–2085, 2015.
- [32] X. Liang, X. Gong, Y. Wu, D. W. K. Ng, and T. Hong, "Analysis of outage probabilities for cooperative noma users with imperfect csi," in *2018 IEEE 4th Information Technology and Mechatronics Engineering Conference (ITOEC)*, 2018, pp. 1617–1623.
- [33] M. Pratesi, F. Santucci, and F. Graziosi, "Generalized moment matching for the linear combination of lognormal rvs: application to outage analysis in wireless systems," *IEEE Transactions on Wireless Communications*, vol. 5, no. 5, pp. 1122–1132, 2006.
- [34] I. S. Gradshteyn and I. M. Ryzhik, *Table of integrals, series, and products*. Academic press, 2014.
- [35] M. Abramowitz and I. Stegun, *Handbook of Mathematical Functions with Formulas, Graphs, and Mathematical Tables*, ser. Applied mathematics series. U.S. Government Printing Office, 1972. [Online]. Available: <https://books.google.com.br/books?id=Cxsty7Np9sUC>